EARLY UNIVERSE PHYSICS FROM *COBE*[*]

GEORGE F. SMOOT
Building 50-351 LBL
Lawrence Berkeley Laboratory, Space Sciences Laboratory
and Center for Particle Astrophysics
University of California, Berkeley, CA 94720

ABSTRACT

The *COBE* Differential Microwave Radiometer (DMR) instrument has observed that the full microwave sky is remarkably uniform in the millimeter to centimeter wavelength range. However at a small level ($\sim 10^{-5}$) there is large scale structure. The natural interpretation of this structure is as the imprint of spatial curvature fluctuations, primarily due to density variations, in the early universe. The results are supportive of gravitational instability theories of structure formation and inflation/quantum cosmology models. The natural energy scale for inflation then is $\sim 10^{16}$ *GeV*. A failure to find fluctuations within a factor of two of the *COBE* DMR level would have contradicted gravitational instability models with near scale-invariant spectra.

Presented at the SLAC Summer Institute on Particle Physics,
Stanford, California, July 13 - July 24, 1992

* The *COBE* program is supported by the Astrophysics Division of NASA's Office of Space Science and Applications. This work supported in part by the Director, Office of Energy Research, Office of High Energy and Nuclear Physics, Division of High Energy Physics of the U.S. Department of Energy under Contract No. DE-AC03-76SF00098.

1. INTRODUCTION

The recent *COBE* DMR (Smoot *et al.* 1992) observation of large-angular-scale anisotropy in the Cosmic Microwave Background (CMB) has provided an outline of initial conditions for the formation of large-scale structure and has opened a critical empirical window for testing the inflationary model of the universe. Ten years ago, inflation was found to generate a nearly scale-invariant (Harrison-Zel'dovich) spectrum of energy density fluctuations due to de Sitter fluctuations of the inflaton field (Guth and Pi 1982; Hawking 1982; Starobinskii 1982; Bardeen *et al.* 1983). de Sitter fluctuations are Hawking radiation in an exponentially expanding universe. The scale-invariance of the fluctuation amplitude is a direct result of the constant expansion rate of a de Sitter phase.

The conventional inflationary prediction for how the CMB anisotropy varies with angular scale is that $\Delta T/T$ is independent of angle for angles greater than a few degrees, consistent with the *COBE* DMR measurements to date. Fluctuations on smaller angular scales were already within the observed horizon and already growing prior to decoupling. The prediction for $\Delta T/T$ depends on the amount and the nature (cold, warm, hot) of the dark matter. The fluctuations grow by gravitational accretion into the structure observed in the present epoch – for example, galaxies, clusters of galaxies, and larger structures.

As *COBE* DMR continues its observations, and analysis and measurements at smaller angular scales improve, the tests of the conventional inflationary prediction will become much more precise. Likewise, the definition of the initial conditions will become more precise as will the information about the nature of dark matter and the process of structure formation.

2. MOTIVATION

Contrary to the usual experience of particle physicists, gravity is thought to be the dominant force in the universe on large scales and at ultrahigh energies. Particle theorists speculate that at the Planck energy scale all forces unify at equal strength. General relativists hold that the structure of space-time is directly connected to the matter and energy content through gravity. The first role of gravity is the definition of the geometry of the universe. The second role of gravity is to form and hold together large scale structures made of matter. Galaxies and clusters of galaxies are examples.

Astronomers have long assumed that all objects of planetary size and larger are held together by gravity, and that these structures formed through gravitational instability. A very nearly uniform distribution of matter under the influence of gravity will soon clump.

A clump quickly virializes so that its kinetic energy matches its potential energy. By measuring the characteristic velocities and the physical scale of the system and using Newton's law of gravitation, one can determine the enclosed gravitational mass. When this is done on galactic, binary galaxy, galactic cluster scales and more loosely using large-scale velocity flows, one finds as the physical scale increases the ratio of dark to light mass increases from about 10 to about 100.

Other astronomers are looking at the gravitational bending of light due to the general relativistic effect of matter (stress-energy) curving space and thus the

apparent bending of light traveling on its geodesic. Gravitational lenses are a manifestation of this effect, demonstrating that quasars and young blue galaxies are behind more evolved galaxies and allowing determination of the mass of the intervening galaxy. Recently, a new area has opened as researchers use galactic clusters and look for the lensed arcs of the distant faint blue galaxies. Bernard Fort and Valerie de Lapparant of Toulouse, Tony Tyson of Bell Labs and their respective colleagues have given beautiful presentations on this new field. We will all marvel over the progress in the field and how we are really getting to the point of testing the effects of gravity on really large scales and how everything seems to hang together. We can expect many more interesting results in this area.

Gravitational instability theories of structure formation start with very small amplitude inhomogeneities in an otherwise uniform matter distribution. The regions of relative overdensity attract nearby material and the density contrast ($\delta\rho/\rho$) grows. In a static universe the growth is exponential. In an expanding universe the growth is slowed to be linear with the expansion factor ($1+Z$, where Z is the redshift). In the early universe the high intensity of the Cosmic Background Radiation (CBR) keeps ordinary baryonic matter from clumping before a redshift of about 10^3. Thus at that epoch the density variations must have been about $\delta\rho/\rho \geq 10^{-3}$ for the density contrast to have grown to order unity ($\delta\rho/\rho \approx 1$) by the present time so that non-linear effects could become important and bound systems could have formed.

Gravitational instability theories with non-baryonic dark matter can accommodate a factor of 10 smaller initial density contrast variations and, thus, CBR temperature fluctuations. The key is that the dominant matter in the universe not interact electromagnetically. At early epochs the energy density in photons dominates matter gravitationally and prevents any clumping. When the matter energy density exceeds the photon energy density at a redshift of about 10^4, the non-electromagnetically interacting matter can begin clumping through gravitational instability. The electromagnetically interacting matter – a highly ionized medium primarily composed of electrons and protons – is prevented from clumping because of the drag imposed by the CBR photons Thomson scattering with the electrons. Once the temperature of the cosmic background falls below the ionization threshold the newly formed neutral atoms can begin clumping. If the non-baryonic matter has already begun clumping, those regions provide seeds for enhanced structure formation. The more the non-baryonic matter dominates the matter density of the universe, the more important the effect.

Density variation in the early universe produces gravitational potential variations resulting in fractional temperature anisotropy in the CBR on the order of one third of the fractional density variation: $\delta T/T \approx 1/3\ \delta\rho/\rho$ (Sachs and Wolfe 1967). The *COBE* DMR experiment was designed to look for these fluctuations and gravity's influence on the large scale structure of the universe and its subsequent evolution. Since we knew that the effect of these density perturbations would be small, quite small as it turned out, we had to design the experiment carefully to ensure stability and to avoid potential systematic effects.

The Cosmic Background Explorer (*COBE*)** science team of six members was put together by NASA from members of three groups proposing three cosmological

** *COBE* is a NASA scientific satellite. Goddard Space Flight Center (GSFC), with the scientific guidance of the *COBE* Science Working Group, is responsible for the development and operation of *COBE*.

experiments in response to a space mission opportunity announced in 1974. The original six *COBE* science team members grew to 19 over the years and each of the three *COBE* instruments developed its own team of scientists, engineers, and other technical personnel. Over the years very many people contributed to the success of *COBE* and the DMR instrument. The *COBE* science working group is composed of C. L. Bennett, N. W. Boggess, E. S. Cheng, E. Dwek, S. Gulkis, M. G. Hauser, M. Janssen, T. Kelsall, P. Lubin, J. Mather, S. S. Meyer, S. H. Moseley, T. Murdock, R. Schafer, R. F. Silverberg, G. F. Smoot, R. Weiss, D. Wilkinson, and E. L. Wright, and each is a co-investigator on all three instruments. The DMR team also currently includes J. Aymon, A. Banday, G. De Amici, G. Hinshaw, A. Kogut, E. Kaita, C. Lineweaver, K. Loewenstein, P. D. Jackson, P. Keegstra, R. Kummerer, J. Santana, and L. Tenorio. It is through these people and their predecessors and the others that worked on *COBE* that the DMR has been able to achieve a sensitivity $\delta T/T$ on the order of 10^{-6}. Four people, Chuck Bennett, Al Kogut, George Smoot, and Ned Wright, led the effort to publish the current results and are the first authors of the four papers presenting the results announced in April 1992.

3. *COBE* DMR EXPERIMENT OVERVIEW

The Differential Microwave Radiometers (DMR) instrument (Smoot 1990) aboard NASA's Cosmic Background Explorer (*COBE*) satellite was designed to provide precise maps of the microwave sky on large angular scales, limited only by instrument sensitivity and observation time. The DMR consists of six differential microwave radiometers, two independent radiometers at each of three frequencies: 31.5, 53, and 90 GHz (wavelengths 9.5, 5.7, and 3.3 mm). These frequencies encompass a window in which the CBR dominates foreground galactic emission by at least a factor of roughly 1000. The multiple frequencies combined with data from other experiments allow subtraction of galactic emission using its spectral signature, yielding maps of the CBR and thus the distribution of matter and energy in the early universe.

COBE was launched on a Delta rocket into near-polar orbit on 18 November 1989 and has been taking DMR data ever since (Boggess *et al.* 1992). The *COBE* mission was designed to allow very precise and accurate observations. The near-terminator, sun-synchronous 99° inclination orbit provides full sky coverage in six months and a very sheltered environment for the instruments.

Each radiometer measures the difference in microwave power between two regions of the sky separated by 60°. The combined motions of spacecraft spin (75 second period), orbit (103 minute period), and orbital precession (1° per day) compare each sky position to all others through a massively redundant set of all possible difference measurements spaced 60° apart.

A software analysis system receives data telemetered from the *COBE* satellite, determines the instrument calibration, and inverts the difference measurements to map the microwave sky in each channel. Although the experiment has been designed to minimize or avoid sources of systematic uncertainty, both the instrument and the data processing can potentially introduce systematic effects correlated with antenna pointing, which would create or mask features in the final sky maps. The following sections discuss the DMR's ability to distinguish systematic artifacts from cosmological signals, present results from the first year of operation, and discuss

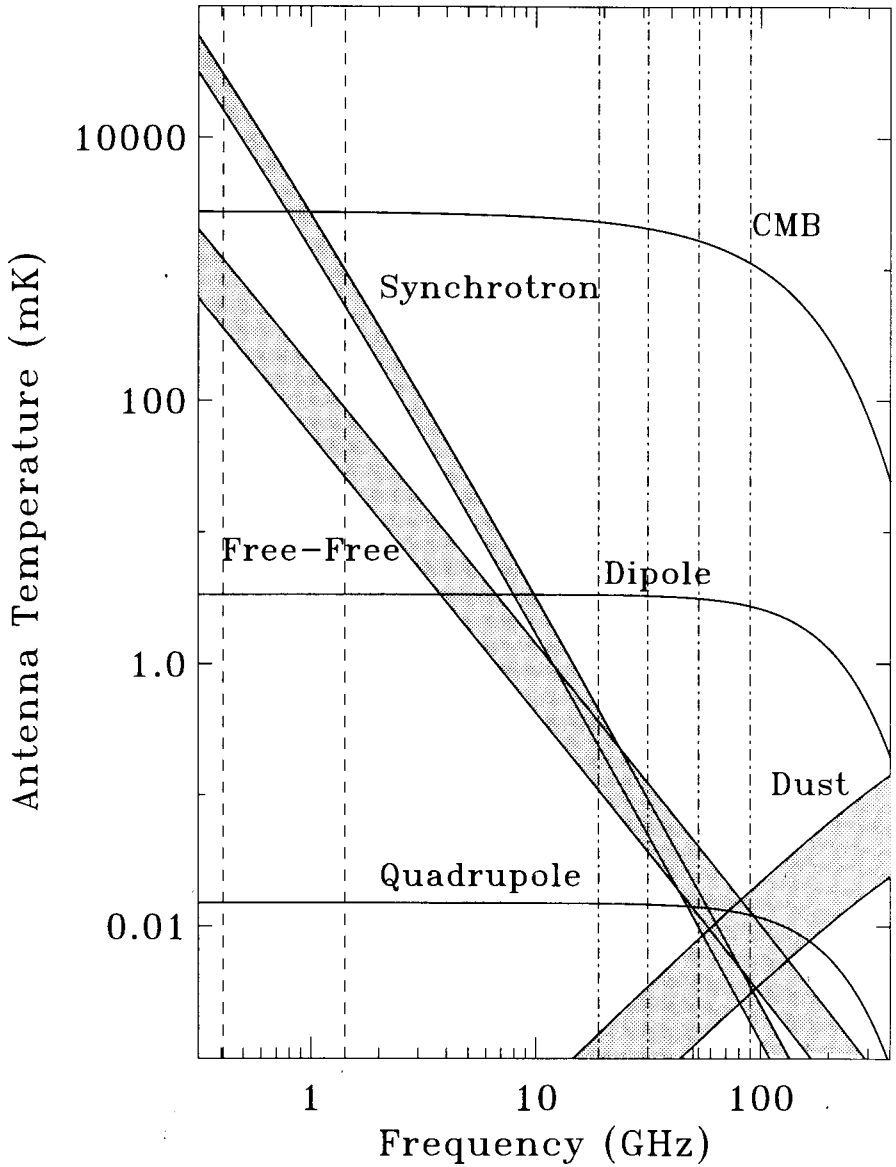

some implications of these results for cosmology.

4. LIMITS ON POTENTIAL SYSTEMATICS

The sky maps may in principle contain contamination from local sources or artifacts from the data reduction process. The data reduction and analysis process must distinguish cosmological signals from a variety of potential systematic effects. These can be categorized into several broad classes (Kogut *et al.* 1992) listed in Table I.

The most obvious source of non-cosmological signals is the presence of foreground microwave sources in the sky. These include thermal emission from the *COBE* spacecraft itself, from the earth, moon, and sun, and from other celestial objects. Non-thermal radio-frequency interference (RFI) must also be considered, both from ground stations and from geosynchronous satellites. Although the DMR instrument is largely shielded from such sources, their residual or intermittent effect must be considered.

A second class of potential systematics may result from the changing orbital environment on the instrument. Instrument characteristics vary slightly with changes in temperature, voltage, and local magnetic field, each of which is modulated by the *COBE* orbit. Longer-term drifts can also affect the data. Finally, the data reduction process may introduce or mask features in the data. The DMR data are differential; the map algorithm is subject to concerns of both coverage (closure) and solution stability. Other features of the data reduction, particularly the calibration and baseline subtraction, are also a source of potential artifacts.

TABLE I. Major Classes of Potential Systematic Effects.

Class / Effect	Typical 95% CL Limit (μK)
Foreground Emission	
Earth	0.7
Moon	0.1
Sun	0.4
Planets (Jupiter)	0.2
RFI	0.0
COBE Shield	0
Zodiacal Dust	0
Environmental Susceptibilities	
Magnetic	1.9
Thermal	1.5
Voltage	0.1
COBE Cross-talk	1
Miscellaneous	5
Processing and Software Artifacts	
Absolute Calibration	2
Calibration Drifts	0
Antenna Pointing	0
Solution Stability	0.1
Noise Properties	0.1
Confusing Sources	
Galactic Emission	3
Extragalactic Radio Sources	1-2

All potential sources of systematic error must be identified and their effects measured or limited before maps with reliable uncertainties can be produced. A variety of techniques exist to identify potential systematics and place limits on their effects. For known celestial sources or geosynchronous RFI, the mapping program can produce a sky map in appropriate object-centered coordinates. The contribution of a source at a given distance from beam center can be read directly from the maps to the noise limit. Spike detection and direct inspection of the data during satellite telemetry transmission limit the effects of asynchronous or intermittent RFI.

Each real and potential systematic effect has been treated in at least two of the ways listed in Table II and the results summarized in Kogut *et al.* (1992).

TABLE II. Tests for Systematic Effects and Understanding of Instrument.

Chopping at several time scales: spin period (75 s); orbit period (102 min); seasonal (6 months).
Instrument response (gain, beam pattern, etc.): characterized before flight; cross-checked in flight.
Multiple cross-checks for each known effect.
Generic tests for unknown effects.
Specific techniques: apply modeled correction; fit specific model to time-ordered data; fit generic model to time-ordered data; rebin data in source-fixed coordinates; bin data at the spin and orbit periods; fourier transform the data; compare maps with and without suspected effect; and Monte-Carlo simulations.

5. *COBE* DMR RESULTS

The first-year data have been processed to produce maps of the microwave sky for each of the six DMR channels. The independent maps at each frequency enable celestial signals to be distinguished from noise or spurious features: a celestial source will appear at identical amplitude in both maps. The three frequencies allow separation of cosmological signals from local (galactic) foregrounds based on spectral signatures. The maps have been corrected to solar-system barycenter and do not include data taken with an antenna closer than 25° to the moon; no other systematic corrections have been made. All six maps clearly show the dipole anisotropy and galactic emission. The dipole appears at similar amplitudes in all maps while galactic emission decreases sharply at higher frequencies, in accord with the expected spectral behavior.

Motion with velocity β = v/c relative to an isotropic radiation field of temperature T_o produces a Doppler-shifted temperature

$$T(\theta) = T_o(1-\beta^2)^{1/2}/(1-\beta\cos(\theta)) \approx T_o\,(1+\beta\cos(\theta) + (\beta^2/2)\cos(2\theta) + \mathrm{O}(\ \mathrm{beta}^3)).$$

The first term is the monopole CBR temperature without a Doppler shift. The term proportional to β is a dipole, varying as the cosine of the angle between the velocity and the direction of observation. The term proportional to β^2 is a quadrupole, varying as the cosine of twice the angle with amplitude reduced by 1/2 β from the dipole amplitude.

The DMR maps clearly show a dipole distribution consistent with a Doppler-shifted thermal spectrum. The DMR finds the same thermodynamic amplitude at all three frequencies. Using the DMR direction and FIRAS spectrum one finds that the difference in spectra taken near the hot and cold poles is described to better than 10% by the difference in blackbody spectra. The DMR maps are well-fitted by a dipole cosine dependence, with an annual modulation by the 30 km/s earth orbital velocity. Everything is consistent with a kinematic effect of our motion relative to the CMB rest frame and thus Doppler-shift origin.

The implied velocity for the solar-system is $\beta = 0.00123 \pm 0.00003$ towards $(\alpha, \delta) = (11.2^{\mathrm{h}} \pm 0.2^{\mathrm{h}}, -7° \pm 2°)$, or $(l, b) = (265° \pm 2°, 48° \pm 2°)$. The solar system velocity with respect to the local standard of rest is about 20 km/s toward $(l, b) = (57°, 23°)$, while galactic rotation moves the local standard of rest at 220 km/s toward (90°, 0°) (Fich, Blitz, and Stark 1989). The DMR results thus imply a peculiar velocity for the galaxy of $v_g = 550 \pm 10$ km/s in the direction $(266° \pm 2°, 30° \pm 2°)$ consistent with an independent determination of the velocity of the local group, $v_{lg} = 507 \pm 10$ km/s toward $(264° \pm 2°, 31° \pm 2°)$ (Kerr and Lyndon-Bell 1990; Yahil, Tamman, and Sandage 1977).

A summation of gravitational attractors in the local area (redshift < 6000 km/s) find reasonable agreement between a gravitationally induced velocity and the CMB dipole magnitude and direction (e.g., Bertschinger *et al.* 1990).

For the DMR maps with the best-fitted Doppler effect removed from the data, the only remaining high signal-to-noise ratio large-scale feature is galactic emission, confined to the plane of the galaxy. This emission is consistent with emission from electrons (synchrotron and HII) and dust within the galaxy. When one analyzes the maps more thoroughly other features become apparent. A natural question is: are the features galactic? We have studied galactic emission and the features,

and conclude that the effect is not due to galactic emission as we understand it at the present time (Bennett *et al.* 1992). There might be classes of emitters which have not yet been detected or have a much different spatial distribution of emission than observed at other frequencies, or a net conspiracy of the three major sources of galactic emission: synchrotron, free-free, and dust, to alias a thermal spectrum. This is fairly unlikely.

Extragalactic radio sources are expected to produce variations in the DMR beam of about 1 to 2μK. Less is expected from infrared sources. Again one might envision a new class of emitters or effects.

There is evidence of other features. These include a quadrupole anisotropy and anisotropy at higher order spherical harmonics. We have made a series of spherical harmonic fits to the data, excluding data within several ranges of galactic latitude. The quadrupole and higher-order terms are limited to $\delta T/T < 10^{-5}$. However, there are statistically significant features at slightly lower levels. The best-fitted amplitude for the observed rms quadrupole amplitude was $13 \pm 4\mu$K corresponding to $\delta T/T \approx 5 \times 10^{-6}$. The rms fluctuations on a 10° angular scale were found to be $30 \pm 5\mu$K corresponding to $\delta T/T \approx 1.1 \times 10^{-5}$.

The correlation function, $C(\alpha) = < T(n_1)T(n_2) >$, is the average product of temperatures separated by angle α. It is calculated for each map or in crosscorrelation between maps by multiplying all possible pixel pairs outside a galactic latitude cut, typically 20°, and averaging the results into 2.6° bins after removing the least squares fitted mean, dipole, and quadrupole. The correlation function is related to the sky temperature power spectrum

$$C(\alpha) = \sum_{l>2} \Delta T_l^2 W(l)^2 P_l(\cos\alpha), \quad \Delta T_l^2 = \frac{1}{4\pi} \sum_m |a_{lm}|^2,$$

where P_l are the Legendre polynomials, and $W(l) = \exp[-1/2(l(l+1)/17.8^2)]$ is the weighting function for the DMR 3.2° rms Gaussian beam, ΔT_l^2 is the rotationally-invariant multipole moment power, and the a_{lm} are the spherical harmonic coefficients according to the relation

$$T(\theta,\phi) = \sum_l \sum_{m=-l}^{l} a_{lm} Y_{lm}(\theta,\phi).$$

If one has a model of the primordial (or surface of last scattering) fluctuations which predicts the power spectrum of fluctuations, then one can readily calculate the model correlation function $C(\alpha)$ and compare it to the DMR correlation function. A particularly interesting version is the scale-free power spectrum - a power law in physical size or angle.

A major finding is that the fluctuations are well fitted by a normally-distributed, scale-invariant spectrum. With the dipole and quadrupole removed from the data the best-fitted scale-free spectrum has an equivalent rms quadrupole amplitude of $16 \pm 4\mu$K and a power-law index of 1.1 ± 0.6 compared to 1 for a scale-invariant spectrum. Similarly, a search for non-Gaussian fluctuations on the sky showed no features to $\delta T/T < 8 \times 10^{-5}$. The results are insensitive to the precise cut in galactic latitude and are consistent with the expected Gaussian instrument noise and scale invariant fluctuations. The reported uncertainties are 95% confidence level unless otherwise stated, and include the effects of systematics as listed in Table I.

The *COBE* DMR measurement of CBR anisotropies provides significant new information on the formation of large-scale structure and limits to the dynamics and physical processes in the early universe. The dipole anisotropy provides a precise measure of the earth's peculiar velocity with respect to the comoving frame. The results confirm some of the major predictions of inflation, namely the prediction of normally-distributed, nearly scale-invariant fluctuations (Bardeen, Steinhardt, and Turner 1982; Guth and Pi 1982; Hawking 1982; Starobinskii 1982).

Since we do not believe the observation is due to an instrumental or experimental effect, a local source, our galaxy or other galaxies, the next step is the cosmological interpretation of the results. We make the assumption that the large-scale structure observed is primarily due to effects at the surface of last scattering, i.e., about one optical depth for Thomson scattering.

6. INTERPRETATION

A major DMR goal is to investigate the large-scale structure and evolution of the universe and the physics occurring in the early universe.

6.1 Geometry of the Universe

The DMR observations of full sky CBR isotropy imply that the large scale geometry of the universe is given by the Robertson-Walker metric (Ehlers, Geren, and Sachs 1968).

6.1.1 Gravity Waves

One metric perturbation is gravitational radiation. Local long-wavelength gravitational waves distort the metric and produce a quadrupole temperature variation in the CBR (Burke 1975). The limits $\delta T/T < 0.9 \times 10^{-5}$ for quadrupole imply that the energy density of a single plane wave of wavelength λ_{gw} is

$$\Omega_{gw} < 0.3 \times 10^{-10}[\frac{c/H_o}{\lambda_{gw}}]^2 = 3 \times 10^{-6}(\frac{\lambda_{gw}}{10\ Mpc})^{-2}h^{-2}\ ,$$

$$\Omega_{gw} < \frac{1}{3}[\frac{c/H_o}{\lambda_{gw}}]^2[\frac{\delta T}{T}]^2 < 0.3 \times 10^{-10}[\frac{c/H_o}{\lambda_{gw}}]^2 = 3 \times 10^{-6}(\frac{\lambda_{gw}}{10\ Mpc})^{-2}h^{-2}$$

where Ω_{gw} is the energy density of the radiation divided by the critical density, λ_{gw} is the wavelength at the current epoch, and h is $H_o/100\mathrm{kms}^{-1}\mathrm{Mpc}^{-1}$.

A chaotic superposition of gravity waves has 8/5 greater energy density.

Gravity waves on the surface of last scattering will generate chaotic fluctuations. The DMR is sensitive primarily to gravitational waves with scale sizes $\geq 7°$ at the surface of last scattering, or 400 Mpc today. The finite thickness of the surface of last scattering washes out the effect of gravity waves with comoving wavelengths less than about 100 Mpc ($\theta \approx 1°$) (Linder 1988). The measured anisotropy, $\delta T/T$, limits the current energy density of scale:

$$\Omega_{gw-ls} < 1/3[\frac{\delta T}{T}]^2 \approx 3 \times 10^{-11}\ .$$

6.1.2 Density Perturbations

Another metric perturbation of interest for gravitational instability models of large-scale structure formation are density perturbations. This is the standard interpretation of the DMR observations - see below.

6.1.3 Topological Defects

Cosmic strings are stable, nearly one-dimensional defects which are very thin lines of a higher energy vacuum state. Cosmic strings are characterized by their mass per unit length μ. Many authors have calculated the anisotropy produced by various configurations of cosmic strings, with typical values (Vilenkin 1985; Stebbins 1988; Stebbins *et al.* 1987)

$$\frac{\delta T}{T} \approx 8\pi\beta\gamma\frac{G\mu}{c^2} \quad .$$

The DMR experiment limits large-scale cosmic strings to $G\mu/c^2 < 3 \times 10^{-6}$.

Domain walls are stable, nearly two-dimensional, defects which are very thin sheets of a higher energy vacuum state. If they persist from early times, the domain walls dominate the universe. Thus we only consider late-time phase transitions in which the energy density per unit area in the walls, σ, is relatively small. CBR photons passing through a domain wall undergo a frequency shift. The general pattern is a rotationally symmetric cusp with maximum anisotropy amplitude about $\pi G\sigma/H_o$ (Stebbins and Turner 1989; Turner, Watkins, and Widrow 1991). The lack of apparent cusps in the DMR maps limits $\sigma < 10\mathrm{MeV}^3(\approx 4.6 \times 10^{-5}$ gm/cm^2).

Textures are unstable three-dimensional defects and their effects come from thin sheets where there is a high gradient caused by the change from one phase to another of the zero energy vacuum state. The metric perturbations produced by collapsing knots of global texture is calculated to be a collection of various-sized red and blue shifted disks covering about 10% of the sky.

If textures seed the formation of large-scale structure, there should be about 10 disks with radius $\sim 8°$ and anisotropy amplitude $|\delta T/T| > 2 \times 10^{-4}$ (Gooding, Spergel, and Turok 1991; Park, Spergel, and Turok 1991; Spergel, Turok, Press, and Ryden 1991). These textures would be detectable. We see no evidence for fluctuations on a 10° scale larger than $|\delta T/T| \approx 8 \times 10^{-5}$.

There is no evidence for topological defects such as cosmic strings, domain walls, and textures. The large-scale geometry of the universe appears to be uniform and without defects.

6.2 Dynamics of the Universe

6.2.1 Rotation of the Universe

The anisotropy results constrain global shear and vorticity in the early universe. If the universe were rotating (in violation of Mach's Principle), the resultant metric would cause null geodesics to spiral. In a flat universe, the anisotropy is dominated by a quadrupole term (Collins and Hawking 1973; Barrow, Juskiewicz, and Sonoda 1985). The DMR results limit the shear to $\sigma/H_o < 10^{-6}$ and the global rotation of the universe to $\omega/H_o < 10^{-6}$, or less than one ten-thousandth of a turn in the last ten billion years. This is less than is needed as primordial vorticity to cause the rotation of galaxies.

6.2.2 Expansion of the Universe

If the expansion of the universe were not uniform, the expansion anisotropy produces a temperature anisotropy in the CBR of similar magnitude. The DMR-measured isotropy indicates that the Hubble expansion is uniform to better than one part in 10^5.

6.3 Observational Tests of Inflation

The inflationary paradigm is central to our modern theory of cosmology. It solves the flatness and horizon problem. It cleans out the early relics and provides a mechanism for producing large scale structure. How can it be tested? There are a number of predictions of inflation that are central to the paradigm. For example, the universe should be flat. One original motivation for inflation is the overall CBR isotropy. The isotropy limits have improved by about a factor of ten since inflation was first proposed as a solution, and the flatness of the universe and inflation thus remains a valid explanation today. However, inflation does predict that there should be some perturbations that appear and some that do not. The next sections discuss some of these perturbations and their effect on the CMB, and how the DMR observations compare.

6.3.1 Rotation - Vorticity and Shear

In order for the inflationary epoch to occur, the energy density in vorticity and shear must be less than the kinetic energy at the Planck scale. As the universe expands during inflation the energy density in shear and vorticity must decrease to conserve angular momentum. During inflation the expansion rate remains nearly constant ($H \approx$ constant). As a result inflation decreases shear and vorticity relative to the expansion rate so that ω/H and σ/H will be below 10^{-7}. The DMR limits, in that sense, support inflation and Mach's Principle.

6.3.2 Relic Gravitons

Inflationary models predict that the zero point quantum fluctuations produce relic gravitons with a Harrison-Zeldovich strain spectrum of amplitude $A_{graviton} = 2/\pi^{1/2} H/M_{Planck}$ (Abbott and Wise 1984). These gravitons will produce CBR temperature fluctuations of order $\delta T/T \approx H/M_{Planck}$, where H is the Hubble parameter during inflation. As a result, the magnitude of the Hubble parameter, H, near the end of the inflationary stage is restricted by the anisotropy limits.

The energy density of gravitons in units of the critical density is

$$\Omega_{graviton} = 10^{-4}(M/M_{Planck})^4$$

for wavelengths significantly smaller than the horizon, rising to $\rho_{vac}/M^4_{Planck} = (M/M_{Planck})^4$ at horizon size. The quadrupole CBR anisotropy and smaller angular scales limits imply $H_{inflation} < 2 \times 10^{-5} M_{Planck}$, the inflation energy scale of interest for our observable universe is far removed from the Planck scale ($M < 10^{17}$ GeV), and the energy density of the vacuum is $\rho_{vac} = M^4 < 10^{-9} M^4_{Planck}$.

One could of course assume that the full anisotropy seen for the quadrupole and higher order moments is due to gravity waves from inflation, and directly measure the energy scale of inflation at about 60 e-foldings from the end of inflation. One finds a value on the order of 10^{16} GeV. However, it is unlikely that most of the

anisotropy would be due to gravity waves from inflation. One expects scalar density fluctuations to be produced also. The ratio of tensor (gravity wave) curvature to scalar (density variation) curvature indicates both the value of the inflation potential and its derivative at the time the fluctuations on our present horizon were produced (Davis *et al.* 1992).

6.3.3 Spectrum of Initial Perturbations

The simplest and most plausible inflation models give fluctuations which are normally distributed and are nearly scale invariant. If these fluctuations account for the structure and large-scale velocity flow observed in the present universe, they must produce small but detectable CBR anisotropies in the present universe (Abbott and Wise 1984; Bond and Efstathiou 1984; Kolb and Turner 1990). We consider the primordial spectrum we report in Smoot *et al.* (1992) in the case of the various gravitational instability models in Wright *et al.* (1992), and show that a number of models give adequately matching predictions. The fluctuations are consistent with a Gaussian distribution and inconsistent with highly non-Gaussian models. In this sense the *COBE* DMR data provide support for the inflationary models of cosmology and restrict the class of viable models of large-scale structure formation.

DMR observations are consistent with inflation but do not necessarily confirm it.

TABLE III. *COBE* DMR Observational Tests of Inflation.

Test	Prediction	Result	Rating
Rotation (vorticity ω)	$\omega/H < 10^{-7}$	$\omega/H < 10^{-6}$	*
Topological Defects	None	$\delta T/T < 8 \times 10^{-5}$ on 7° scales	*
Fluctuations	Gaussian	No Large Tails	*
Power Spectrum	n=1	n=1.1 ± 0.6	**

7. CONCLUSIONS AND FUTURE

An examination of the DMR maps (Smoot *et al.* 1992) reveals that the statistical fluctuations in the map are consistent with instrument noise plus a Gaussianly-distributed power spectrum of structure in the maps. The levels of both the noise and structure are low; however, the information on the properties of the structure impose significant restrictions on possible cosmologies.

The CBR anisotropies on all angular scales $\geq 7°$ to $\delta T/T \leq 10^{-5}$ are consistent with a universe described by a Robertson-Walker metric, inflationary models and gravitational instability, and show no positive evidence of anisotropic expansion, rotation, or defects (strings, walls, texture).

The DMR continues to take data and the team to process it. The DMR has accumulated nearly three years of data and we are far along on processing the second year. We can anticipate that additional data and results are forthcoming.

8. ACKNOWLEDGEMENTS

The *COBE* program is supported by the Astrophysics Division of NASA's Office of Space Science and Applications. This work is supported in part by the Director, Office of Energy Research, Office of High Energy and Nuclear Physics, Division of High Energy Physics of the U.S. Department of Energy under Contract No. DE-AC03-76SF00098.

References

1. Abbott, L. F., and Wise, M. B., 1984, *Astrophys. J. Lett.* **282**, L47.
2. Abbott, L. F., and Wise, M. B., 1984, *Nucl. Phys. B* **244**, 541-548.
3. Bardeen, J. M., Steinhardt, P. J., and Turner, M. S., 1982, *Phys. Rev. D* **28**, 679-693.
4. Barrow, J. D., Juszkiewicz, R., and Sonoda, D. H., 1983, *Nature* **305**, 397-401.
5. Barrow, J. D., Juskiewicz, R., and Sonoda, D. H., 1985, *Mon. Not. R. Astron. Soc.* **213**, 917.
6. Bennett, C. L. *et al.*, 1992, *Astrophys. J.* **396**, L7-L12.
7. Bertschinger, E., Dekel, A., Faber, S. M., Dressler, A., and Berstein, D., 1990, *Astrophys. J.* **364**, 370.
8. Boggess, N. *et al.*, 1992, *Astrophys. J.* **397**, 420-429.
9. Bond, J. R., and Efstathiou, G., 1984, *Astrophys. J. Lett.* **285**, L45.
10. Burke, W. L., 1975, *Astrophys. J.* **196**, 329.
11. Collins, C. B., and Hawking, S. W., 1973, *Mon. Not. R. Astron. Soc.* **162**, 307.
12. Davis, R., Hodges, H., Smoot, G. F., Steinhardt, P., and Turner, M. S., 1992, *Phys. Rev. Lett.* **69**, 1856.
13. Ehlers, J., Geren, P., and Sachs, R., 1968, *J. Math. Phys.* **9**, 134.
14. Fich, M., Blitz, L., and Stark, A., 1989, *Astrophys. J.* **342**, 272.
15. Goetz, G., and Notzold, D., 1990, Fermi Lab preprint.
16. Gooding, A., Spergel, D. N., and Turok, N., 1991, *Astrophys. J.*
17. Gorski, K., 1991, *Astrophys. J. Lett.* **370**, L5.
18. Guth, A., 1981, *Phys. Rev. D* **23**, 347.
19. Guth, A., and Pi, Y-S., 1982, *Phys. Rev. Lett.* **49**, 1110.
20. Hawking, S., 1982, *Phys. Lett.* **115B**, 295.
21. Kerr, F. J., and Lyndon-Bell, D., 1990, *Mon. Not. R. Astron. Soc.* **221**, 1023.
22. Kogut, A. *et al.*, 1992, *Astrophys. J.* **400**.
23. Kolb, E., and Turner, M. S., 1991, *The Early Universe*, Addison Wesley, 383-390, for a good review of gravitational instability and $\delta T/T$.
24. Linder, E., 1988, *Astrophys. J.* **326**, 517.
25. Novikov, I. D., 1968, *Sov. Astron.* **12**, 427-429.
26. Sachs, R. K., and Wolfe, A. M., 1967, *Astrophys. J.* **147**, 73.
27. Schaefer, R. K., 1991, "After the First Three Minutes," eds. Holt, S. S., Bennett, C. L., Trimble, L., AIP.
28. Smoot, G. F. *et al.*, 1990, *Astrophys. J.* **360**, 685.
29. Smoot, G. F. *et al.*, 1991, *Astrophys. J. Lett.* **371**, L1-L5.
30. Smoot, G. F. *et al.*, 1991, *Adv. Space Res.* **11**, No. 2, pp. (2)193-(2)205.
31. Smoot, G. F. *et al.*, 1992, *Astrophys. J. Lett.* **396**, L1-L5.
32. Spergel, D. N., Turok, N., Press, W. H., and Ryden, B., 1991, *Phys. Rev. D* **43**, 1038.
33. Starobinskii, A. A., 1982, *Phys. Lett.* **117B**, 175.
34. Stebbins, A. *et al.*, 1987, *Astrophys. J.* **322**, 1.
35. Stebbins, A., 1988, *Astrophys. J.* **327**, 584.
36. Stebbins, A., and Turner M. S., 1989, *Astrophys. J. Lett.* **329**, L13.
37. Turner, M. S., Watkins, R., and Widrow, L. M., 1991, *Astrophys. J. Lett.* **367**, L43.
38. Turok, N., 1989, *Phy. Rev. Lett.*, **63**, 2625.
39. Turok, N., and Spergel, D., 1990, *Phy. Rev. Lett.* **64**, 2763.
40. Vilenkin, A., 1985, *Physics Reports* **121**, 263.
41. Yahil, A., Tamman, A., and Sandage, A., 1977, *Astrophys. J.* **217**, 903.
42. Wright, E. L. *et al.*, 1992, *Astrophys. J. Lett.* **396**, L13-L18.